Fixed Frequency Integral Sliding Mode Control for Bidirectional Switched Quasi Z-source DC-DC Converter in Standalone PV Connected System

Santhoshkumar Battula
Department of Electrical Engineering
National Institute of Technology
Rourkela, India
b.santhosh226@gmail.com

Man Mohan Garg
Department of Electrical Engineering
Malaviya National Institute of Technology
Jaipur, India
mmgarg.ee@mnit.ac.in

Anup Kumar Panda
Department of Electrical Engineering
National Institute of Technology
Rourkela, India
akpanda@nitrkl.ac.in

Laxmidhar Senapati
Department of Electrical Engineering
National Institute of Technology
Rourkela, India
senapati.laxmidhar321@gmail.com

***Abstract*— Nowadays, energy management in a microgrid consists of distributed renewable energy sources, and distributed energy storage has proven to be a major challenge. The difficulty is successfully managing the dynamic renewable sources, the storage system, and the loads simultaneously. This paper presents a Bidirectional Switched Quasi Z-source DC-DC Converter (BSQZSDC) to integrate an energy storage system with a PV-connected common DC bus. A fixed frequency integral sliding mode controller (FF-ISMC) is used to regulate DC-Link voltage with good dynamic response in the proposed system. The FF-ISMC reduces steady-state errors and provides stable control even when the load changes significantly in both modes operations of BSQZSDC. The controller operates satisfactorily in achieving the voltage regulation objective, as per simulations conducted in MATLAB/Simulink. Finally, the proposed performance of the controller is verified using an experimental setup.**

Keywords— Bidirectional DC-DC Converter (BDC), DC Microgrid, Fixed Frequency Control, Sliding Mode Control (SMC), Quasi Z-source DC-DC Converter (QZSDC).

I. INTRODUCTION

The basic boost converters have traditionally been used to step-up voltages. However, their gain is typically insufficient due increased stress on switches. Hense high gain DC-DC converters came into the limelight. The Z-source (ZS) network is proposed in [1]. It can provide high gain with a moderate duty, and it has ability to use a shoot-through state. The ZS was first used as a Z-source inverter (ZSI) for renewable applications. The Quasi Z-Source Inverter (QZSI) had been proposed in [2]–[4]. The QZSI provides all of the benefits of ZSI. In addition, it delivers continuous input current, which is not in ZSI.

The ZS and QZS also used as DC-DC converters [5], [6]. In [7], [8] describes a BSQZSDC. Individual mode operations are examined in these articles by regulating output voltage. The grid side capacitor voltage must be regulated in both the modes.

To regulate grid-side voltage, different control methods are used. The traditional proportional-integral (PI) approaches are usually implemented [9], [10]. However, with large perturbations, the transient behaviour of these systems is inadequate. This is because small-signal model for each operational point is incorrect. Several nonlinear controllers are used to solve this problem in power electronic converters [11], [12].

The SMC is an approach that can handle parameter changes, external, and internal disturbances more effectively. The hysteresis modulation SMC (HM-SMC) presented in [13], [14] suffers from chattering and frequency variation under disturbances in system. Later, fixed-frequency SMC advanced by using PWM in [15]–[17], which has the advantage of maintaining the constant frequency. While using SMC with PWM, a significant SSE is generated [18], [19]. The proposed FF-ISMC is a method that reduces steady-state error by introducing an integral term of the sum of errors to the SMC.

The design and execution of an FF-ISMC for BSQZSDC is major contributor to the paper. The controller scheme is designed in such that the DC grid voltage is controlled for load variations.

In section II, the analysis and mathematical model of BSQZSDC are presented. The FF-ISMC is analyzed in section III. The simulation and hardware results are presented in section IV, then conclusions in V.

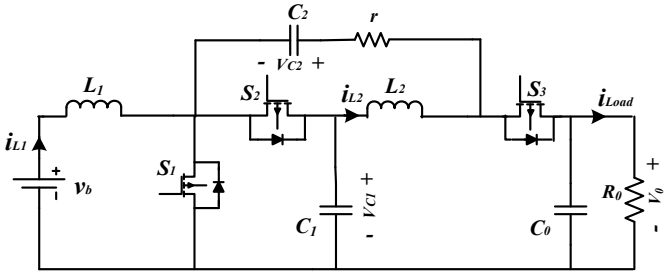

Fig.1. Circuit Diagram of proposed BSQZSDC

II. SYSTEM CONFIGURATION AND MODELLING

The BSQZSDC architecture is given in Fig 1. Three active switches, S_1, S_2, and S_3, make up the topology. By properly choosing the switching signals, the converter can charge and discharge the battery. The operation of the BSQZSDC in boost mode (step-up) is only analyzed in this paper. However, buck mode can also be operated similarly. Switch S_1 works as a primary switch in the boost mode of the BSQZSDC, whereas S_2 and S_3 are complimentary switches to S_1. The V_b is considered to be constant. To

978-1-6654-7350-7/22/$31.00 ©2022 IEEE

avoid complexities in determining the state equations, the ESR, r of C_2, is considered.

BSQZSDC is assumed to operate in CCM, with a constant switching frequency f and a switching input u. The BSQZSDC analyzed by individually observing the two modes.

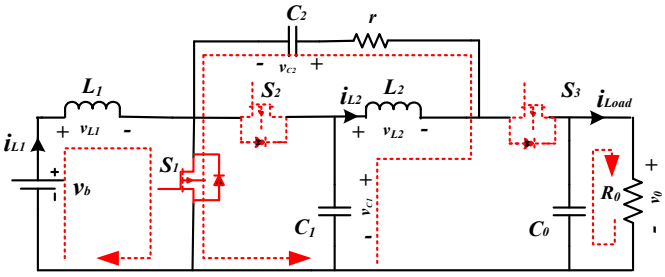

Fig. 2. BSQZSDC in Mode-1.

Mode-1: S_1 is turned ON, S_2 & S_3 turned OFF ($0<t\leq DT$)

In *mode-1*, S_1 is triggerd ON, S_2 and S_3 are triggerd OFF. The circuit can be seen as in Fig.2. After doing an analysis of the circuit, it is possible to deduce that the energy from the battery is being stored in L_1 when switch S_1 is in the ON position. The C_2 is charged by means of the inductor L_2 and the C_1 (which are already charged). Since the load is not directly linked to the battery, the power for the load is provided via the capacitor C_0.

This mode can be modelled in state-space using the basic circuit laws shown:

$$v_{L1} = L_1 \frac{di_{L1}}{dt} = v_b \tag{1}$$

$$v_{L2} = L_2 \frac{di_{L2}}{dt} = v_{C1} - v_{C2} - i_{L2} r \tag{2}$$

$$i_{C1} = C_1 \frac{dv_{C1}}{dt} = -i_{L2} \tag{3}$$

$$i_{C2} = C_2 \frac{dv_{C2}}{dt} = i_{L2} \tag{4}$$

$$i_{C_0} = C_0 \frac{dv_0}{dt} = -\frac{v_0}{R_0} = -i_{Load} \tag{5}$$

Mode- 2: S_1 is turned OFF, S_2 & S_3 turned ON ($DT<t\leq T$).

In *mode-2*, S_1 is triggered OFF, S_2 and S_3 are triggered ON. In this state, the energy in the L_1 charges C_1 through S_2. The energy in the inductor L_2 is used to feed the R_0, and the C_2 is discharged simultaneously.

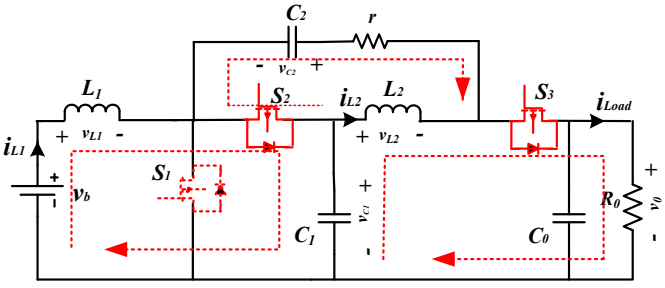

Fig.3. BSQZSDC in Mode-2 ($DT<t\leq T$)

This mode can be modelled in state-space using the basic circuit laws shown as

$$v_{L1} = L_1 \frac{di_{L1}}{dt} = v_b - v_{C1} \tag{6}$$

$$v_{L2} = L_2 \frac{di_{L2}}{dt} = v_{C1} - v_0 \tag{7}$$

$$i_{C1} = C_1 \frac{dv_{C1}}{dt} = i_{L1} - i_{L2} + \frac{v_0 - v_{C1} - v_{C2}}{r} \tag{8}$$

$$i_{C_2} = C_2 \frac{dv_{C_2}}{dt} = \frac{v_0 - v_{C_1} - v_{C_2}}{r} \tag{9}$$

$$i_{C_0} = C_0 \frac{dv_0}{dt} = i_{L_2} - \frac{v_0 - v_{C_1} - v_{C_2}}{r} - \frac{v_0}{R_0} \tag{10}$$

A. State-Model Representation

From equations (1) to (10), the state-space model derived as,

$$\begin{cases} L_1 \dfrac{di_{L_1}}{dt} = v_b - v_{C1}(1-u) \\ L_2 \dfrac{di_{L2}}{dt} = v_{C1} - v_{C2}u - i_{L2}r - v_0(1-u) \\ C_1 \dfrac{dv_{C1}}{dt} = -i_{L2} + \left(i_{L1} + \dfrac{v_0 - v_{C1} - v_{C2}}{r} \right)(1-u) \\ C_2 \dfrac{dv_{C2}}{dt} = i_{L2} + \dfrac{v_0 - v_{C1} - v_{C2}}{r}(1-u) \\ C_0 \dfrac{dv_0}{dt} = -\dfrac{v_0}{R_0} + \left(i_{L2} - \dfrac{v_0 - v_{C1} - v_{C2}}{r} \right)(1-u) \end{cases} \tag{11}$$

where u control input of S_1.

III. Fixed Frequency Integral Sliding Mode Control

The error in i_{L1} and the error in v_0 are control state variables in a fixed-frequency SMC. To reduce steady-state error, a new state variable that is the sum of the v_0 error and the i_{L1} error has been added. Using voltage error, the reference current (i_{ref}) for inductor L_1 is generated (12).

$$i_{ref} = K(v_{ref} - v_0) \tag{12}$$

A. Sliding surface

The FF-SMC contains errors in output voltage, and inductor currents are taken as control sliding variables. Integral of sum of above variables taken as another sliding variable to reduce the steady-state error.

The SMC state variables are given by

$$\begin{cases} x_1 = i_{ref} - i_{L1} \\ x_2 = v_{ref} - v_0 \\ x_3 = \int (x_1 + x_2) dt \end{cases} \tag{13}$$

The proposed controller sliding surface S is defined as

$$S = \alpha_1 x_1 + \alpha_2 x_2 + \alpha_3 x_3 \tag{14}$$

Here $\alpha_1, \alpha_2, \alpha_3$ are the sliding coefficients. Using (13), the dynamic model of BSQZSDC developed as

$$\begin{cases} \dot{x}_1 = -K\dfrac{i_{C_0}}{C_0} - \dfrac{1}{L_1}\left(V_b - v_{C1}(1-u)\right) \\ \dot{x}_2 = \dfrac{-i_{C_0}}{C_0} \\ \dot{x}_3 = x_1 + x_2 \end{cases} \tag{15}$$

v_b is the battery voltage. i_{C0} is the output capacitor current. The FF-ISMC control input is obtained by solving $dS/dt = 0$.

Which gives

$$u_{eq} = \frac{v_{C1} - v_b + k_1\left(V_{ref} - v_0\right) - k_2 i_{C0} - k_3 i_{L1}}{v_{C1}} \tag{16}$$

Where $k_1 = \dfrac{\alpha_3 L_1}{\alpha_1}(K+1)$, $k_2 = \dfrac{L_1}{C_0}\left[K + \dfrac{\alpha_2}{\alpha_1}\right]$, $k_3 = \dfrac{\alpha_3 L_1}{\alpha_1}$

Here k_1,k_2, and k_3 are the fixed gains, and u_{eq} is the equivalent control input.

The proposed FF-ISMC is implemented through PWM. For proposed control, the switching function u has the boundary values of 0 and 1.

$$u = \begin{cases} 1, & s > 0 \\ 0, & s < 0 \end{cases} \tag{17}$$

The control logic taken switching function as below, and it is applied to switch S_1, and its complement is applied to S_2, and S_3.

$$u = \frac{1}{2}\left(1 + sign(\dot{S})\right) \tag{18}$$

By equating u_{eq}=d in the control law (16). where d is the duty ratio, the equations of the control law is comparison of a v_c and a v_{ramp}.

$$\begin{cases} v_C = v_{C1} - v_b + k_1\left(V_{ref} - v_0\right) - k_2 i_{C0} - k_3 i_{L1} \\ v_{ramp} = v_{C_1} \end{cases} \tag{19}$$

The BSQZSDC with FF-SMC is shown in Fig.4.

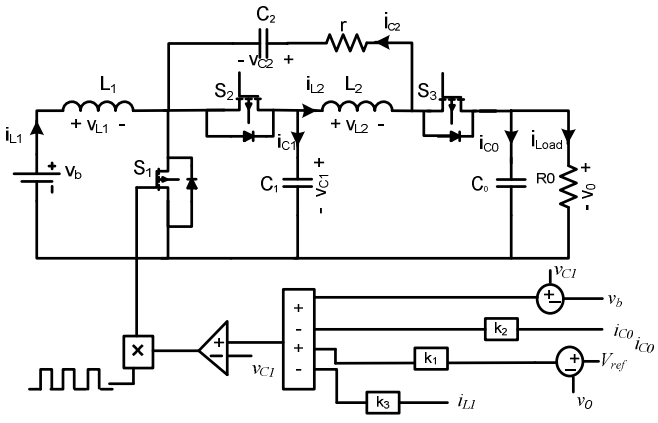

Fig.4. BSQZSDC with FF-ISM controller

B. Existing Conditions

For smooth operation of control, the control logic should satisfy the hitting, existing and stability conditions. The hitting condition has been fulfilled by (17). As for existing condition, the local reachability condition $\lim_{S\to 0} S.dS/dt < 0$, gives

$$\begin{cases} \alpha_1\left[-K\dfrac{i_{C_0}}{C_0} - \dfrac{1}{L_1}\left(V_b\right)\right] - \alpha_2\left[\dfrac{i_{C_0}}{C_0}\right] + \alpha_3\left[x_1 + x_2\right] < 0 \\ \alpha_1\left[-K\dfrac{i_{C_0}}{C_0} - \dfrac{1}{L_1}\left(V_b - v_{C1}\right)\right] - \alpha_2\left[\dfrac{i_{C_0}}{C_0}\right] + \alpha_3\left[x_1 + x_2\right] > 0 \end{cases} \tag{20}$$

If the controller is built using a static sliding-surface that satisfies the requirements for steady-state operation and considers equation (16) into account, then equation (18) can be simplified as

$$\begin{cases} 0 < v_{b(\min)} - k_1\left[V_{ref} - v_{0(SS)}\right] + k_2 i_{C0(\min)} + k_3 i_{L1(Max)} \\ v_{b(\max)} - k_1\left[V_{ref} - v_{0(SS)}\right] + k_2 i_{C0(\max)} + k_3 i_{L1(\min)} < v_{0(SS)} \end{cases} \tag{21}$$

The voltages v_b and v_0 are considered within limit. The boundary values are taken as $v_{b(max)}$,$v_{b(min)}$,$v_{0(max)}$,$v_{0(min)}$. The $i_{L1(max)}$, $i_{L1(min)}$, $i_{C0(max)}$, and $i_{C0(min)}$ are boundary values at full-load conditions. The $v_{C1(SS)}$, and $v_{C2(SS)}$ are steady-state values of v_{C1} and v_{C2}. $v_{o(SS)}$ denotes the expected steady-state output voltage(V_{ref}).

C. Stability Condition

The stability condition can be established by first determining the ideal sliding dynamics of system and then performing an analysis of its equilibrium point.

a) Ideal Sliding Dynamics

Under a large signal model operation, replacing u with u_{eq} in (11), the original BSQZSDC converts the discontinuous system into an ideal SM continuous system,

$$\begin{cases} \dfrac{di_{L1}}{dt} = \dfrac{v_b - v_{C1}}{L_1} + \dfrac{v_{C1}}{L_1}u_{eq} \\ \dfrac{di_{L2}}{dt} = \dfrac{v_{C1} - v_b}{L_2} + \dfrac{v_0 - v_{C2} - i_{L2}r}{L_2}u_{eq} \\ \dfrac{dv_{C1}}{dt} = \dfrac{i_{L1}}{C_1}(1-u_{eq}) - \dfrac{i_{L2}}{C_1} + \dfrac{v_0 - v_{C1} - v_{C2}}{rC_1}(1-u_{eq}) \\ \dfrac{dv_{C2}}{dt} = \dfrac{i_{L2}}{C_2} + \dfrac{v_0 - v_{C1} - v_{C2}}{rC_2}(1-u_{eq}) \\ \dfrac{dv_0}{dt} = \dfrac{-v_0}{C_0 R_0} + \dfrac{i_{L2}}{C_0}(1-u_{eq}) - \dfrac{v_0 - v_{C1} - v_{C2}}{rC_0}(1-u_{eq}) \end{cases} \tag{22}$$

The substitution of (16) into (22) results in equation (23), in which the dynamics of sliding mode controlled BSQZSDC.

b) Equilibrium-point-analysis:

Assume that sliding dynamics will eventually reach a point of equilibrium that will remain stable. The dynamics of system will remain constant at this point of equilibrium if there is no input or loading perturbation (steady-state). At that equilibrium point, equation (23) =0.

$$X_{eq}=\left[\begin{array}{ccccc}\dfrac{V_0^2}{V_b R_L} & \dfrac{V_0}{R_L} & \dfrac{V_{ref}+V_b}{2} & \dfrac{V_{ref}-V_b}{2} & V_{ref}\end{array}\right]^T \tag{24}$$

Where V_b, V_0*, and I_0 are battery voltage, reference output voltage, and output current, respectively.

c) Linearization of ideal Sliding Dynamic:

The linearized dynamic model at equilibrium point (24) had obtained by applying small-signal analysis. Which is shown in (25). In simplified from

$$\frac{d}{dt}X = A_s\hat{X} + B_s\hat{v}_b \tag{26}$$

The characteristic equation is given

$$\left|A_s - \lambda I\right| = 0 \tag{27}$$

The Routh- Hurwitz criteria applied to (27) concluded that the stability conditions are met.

d) Selecting the Sliding coefficients

The sliding coefficients k_1, k_2, and k_3 were chosen based on (21) and observed the effect of changing the control gains.

- Slope of dynamic behaviour of v_0 can be amplified or diminished by varying k_1.
- A little increase in k_2 decreases the settling-time significantly but maximise the SSE.

The values of k_1, *and* k_2, *are* chosen based of observations of system response.

$$\begin{cases}\dfrac{di_{L_1}}{dt}=\dfrac{v_b}{L_1}-\dfrac{v_{C1}}{L_1}\left(\dfrac{v_b-k_1\left(V_{ref}-v_0\right)+k_2i_{C0}+k_3i_{L1}}{v_{C1}}\right)\\ L_2\dfrac{di_{L2}}{dt}=v_{C1}-v_{C2}\left(\dfrac{v_{C1}-v_b+k_1\left(V_{ref}-v_0\right)-k_2i_{C0}-k_3i_{L1}}{v_{C1}}\right)-i_{L2}r-v_0\left(\dfrac{v_b-k_1\left(V_{ref}-v_0\right)+k_2i_{C0}+k_3i_{L1}}{v_{C1}}\right)\\ C_1\dfrac{dv_{C1}}{dt}=-i_{L2}+\left(i_{L1}+\dfrac{v_0-v_{C1}-v_{C2}}{r}\right)\left(\dfrac{v_b-k_1\left(V_{ref}-v_0\right)+k_2i_{C0}+k_3i_{L1}}{v_{C1}}\right)\\ C_2\dfrac{dv_{C2}}{dt}=i_{L2}+\dfrac{v_0-v_{C1}-v_{C2}}{r}\left(\dfrac{v_b-k_1\left(V_{ref}-v_0\right)+k_2i_{C0}+k_3i_{L1}}{v_{C1}}\right)\\ C_0\dfrac{dv_0}{dt}=-\dfrac{v_0}{R_0}+\left(i_{L2}-\dfrac{v_0-v_{C1}-v_{C2}}{r}\right)\left(\dfrac{v_b-k_1\left(V_{ref}-v_0\right)+k_2i_{C0}+k_3i_{L1}}{v_{C1}}\right)\end{cases} \tag{23}$$

$$\begin{cases}\dfrac{d\tilde{i}_{L_1}}{dt}=-\dfrac{\tilde{v}_{C1}}{L_1}\left(\dfrac{V_b+k_1V_0+\tilde{v}_0+k_2\left(-\dfrac{\tilde{v}_0}{R_0}+\tilde{i}_{L_2}\right)+k_3I_{L1}+k_3\tilde{i}_{L1}}{V_{C1}}\right)\\ \dfrac{d\left(I_{L2}+\tilde{i}_{L2}\right)}{dt}=\dfrac{V_{C1}+\tilde{v}_{C1}}{L_2}-\dfrac{V_{C2}+\tilde{v}_{C2}}{L_2}\left(\dfrac{V_{C1}+\tilde{v}_{C1}-V_b+k_1V_0+\tilde{v}_0-k_2\left(-\dfrac{\tilde{v}_0}{R_0}+\tilde{i}_{L_2}\right)-k_3I_{L1}-k_3\tilde{i}_{L1}}{V_{C1}}\right)-\dfrac{\left(I_{L2}+\tilde{i}_{L2}\right)r}{L_2}-\dfrac{\tilde{v}_0}{L_2}\left(\dfrac{V_b-k_1V_0+\tilde{v}_0+k_2\left(-\dfrac{\tilde{v}_0}{R_0}+\tilde{i}_{L_2}\right)+k_3I_{L1}+k_3\tilde{i}_{L1}}{V_{C1}}\right)\\ \dfrac{d\left(V_{C1}+\tilde{v}_{C1}\right)}{dt}=-\dfrac{i_{L2}}{C_1}+\dfrac{1}{C_1}\left(I_{L1}+\tilde{i}_{L1}+\dfrac{V_0+\tilde{v}_0-V_{C1}-\tilde{v}_{C1}-V_{C2}-\tilde{v}_{C2}}{r}\right)\left(\dfrac{V_b-k_1V_0+\tilde{v}_0+k_2\left(-\dfrac{\tilde{v}_0}{R_0}+\tilde{i}_{L_2}\right)+k_3I_{L1}+k_3\tilde{i}_{L1}}{V_{C1}}\right)\\ \dfrac{d\left(V_{C2}+v_{C2}\right)}{dt}=\dfrac{I_{L2}}{C_2}+\dfrac{\tilde{i}_{L2}}{C_2}+\dfrac{V_0+\tilde{v}_0-V_{C1}-\tilde{v}_{C1}-V_{C2}-\tilde{v}_{C2}}{C_2r}\left(\dfrac{V_b-k_1V_0+\tilde{v}_0+k_2\left(-\dfrac{\tilde{v}_0}{R_0}+\tilde{i}_{L_2}\right)+k_3I_{L1}+k_3\tilde{i}_{L1}}{V_{C1}}\right)\\ \dfrac{d\left(V_0+\tilde{v}_0\right)}{dt}=-\dfrac{V_0+\tilde{v}_0}{C_0R_0}+\left(\dfrac{I_{L2}}{C_0}+\dfrac{\tilde{i}_{L2}}{C_0}-\dfrac{V_0+\tilde{v}_0-V_{C1}-\tilde{v}_{C1}-V_{C2}-\tilde{v}_{C2}}{rC_0}\right)\left(\dfrac{V_b-k_1V_0+\tilde{v}_0+k_2\left(-\dfrac{\tilde{v}_0}{R_0}+\tilde{i}_{L_2}\right)+k_3I_{L1}+k_3\tilde{i}_{L1}}{V_{C1}}\right)\end{cases} \tag{25}$$

IV. RESULTS AND DISCUSSION

The FF-ISMC strategy is simulated in MATLAB/Simulink and tested on an experimental prototype. The following subsections will go over these details. The parameters of BSQZSDC are mentioned in Table I.

A. Simulation Results

The load is connected to the common bus of the system, which is connected to a photovoltaic (PV) supply by means of a boost converter interface. It is preferable to have the load maintained at a constant voltage reference of 48V. In the case that the power generated by the PV panel is more than the power required by the load, the BSQZSDC will transition into the buck mode, and the additional power

will be used to charge the battery. In the case that the power from the PV is not sufficient to reach load, the BSQZSDC will switch to boost mode and begin discharging the battery. In the process,battery voltage 12 V taken into consideration, and the reference voltage is chosen at 48V. The photovoltaic (PV) system is simulated as a current source with a supply capacity of 4.17 amps and a power output of 200 watts, and it is linked to the load side of the BQZDC. Observations are made on the performance of the converter under varying loads.

Table I. System Parameters of BSQZSDC

Parameter	**value**
Power	100W
Output Voltage v_0	48 V
Battery voltage v_b	12 V
Inductors L_1, L_2	1mH, 3.3mH
Capacitors $C_1 C_2$	100µF
Resistor r	0.278Ω
Capacitor C_0	470µF

a) Boost Mode (Discharging Mode)

The load power is stepped between 250 W and 300W in boost mode, the FF-SMC is proven to be capable of providing a satisfactory dynamical response to the BSQZSDC in boost mode with a settling-time of around 15 ms with a percentage peak overshoot of 12.5%. The different waveforms of the BSQZSDC are shown in Fig. 5.

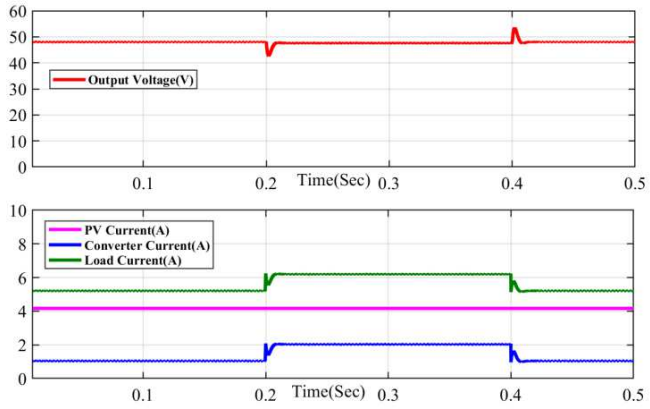

Fig. 5. Simulation results when load power is varied from 250W to 300W and vice-versa (boost mode).

b) Buck Mode (Charging Mode)

In buck mode, the battery begins charging via converter, absorbing the surplus power from PV panels, in order to keep the power balance stable and the v_0 constant. When output power is stepped between 100 W and 200W, the FF-SMC is proven to be capable of providing a satisfactory dynamical response to the BSQZSDC in buck mode with a settling time of 25 ms, and a percentage peak overshoot of 15%. The different waveforms of the BSQZSDC are shown in Fig. 6

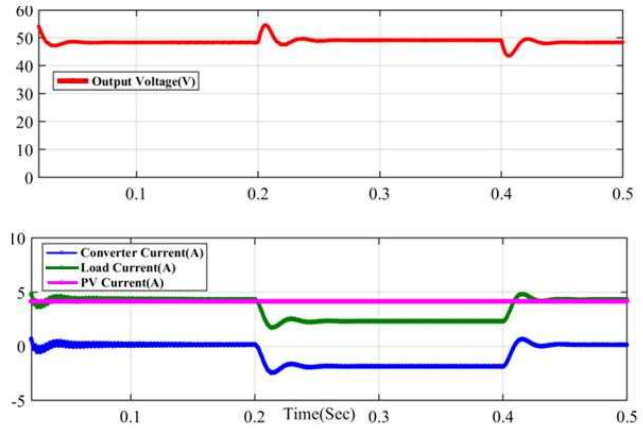

Fig. 6. Simulation results when load power is varied from 200W to 100W and vice-versa (buck mode).

B. Hardware Implementation

The hardware implementation of BSQZSDC converter is shown in Fig. 7.

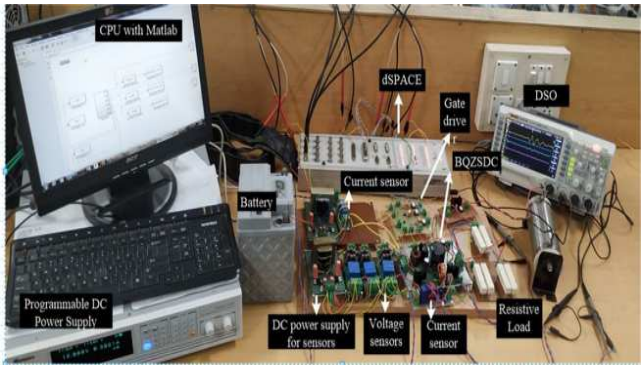

Fig. 7. Experimental setup for proposed work.

A programmable DC-power supply employed as a PV source. 3-Voltage and 2-Current sensors are used. The Dspace-1104 used to implement the FF-ISMC. To capture the results, RIGAL-DS1054 is used.

The battery starts discharging in boost mode, and converter provides the deficit power. As shown in Fig. 7, initial load power is 250W, with the PV source supplying 200W. The controller regulates the v_0 at 48V by supplying the remaining 50W by the battery through the converter.

During the buck mode, the battery starts charging via the converter, which consumes any surplus power to keep power balance. At first, the load power (P_L) is 200W, which is completely manageable for the PV system. As a direct consequence of this, the battery uncharged, and no power is delivered or absorbed. As P_L reduces to 100W, the battery is able to charge itself by using the extra power of 100W, as shown in Fig. 8.

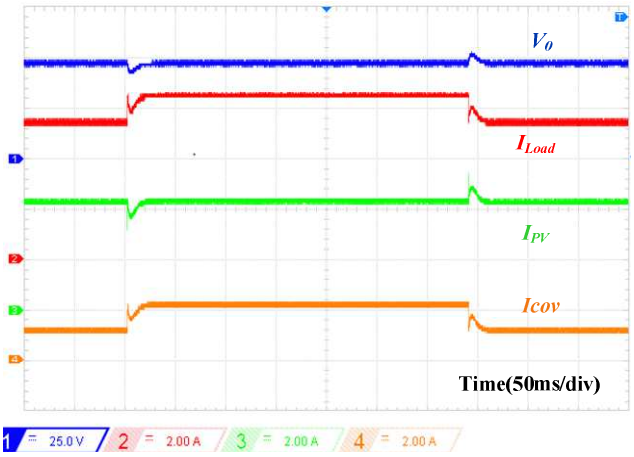

Fig. 7. Experimental results when load power is varied from 250W to 300W and vice-versa (boost mode).

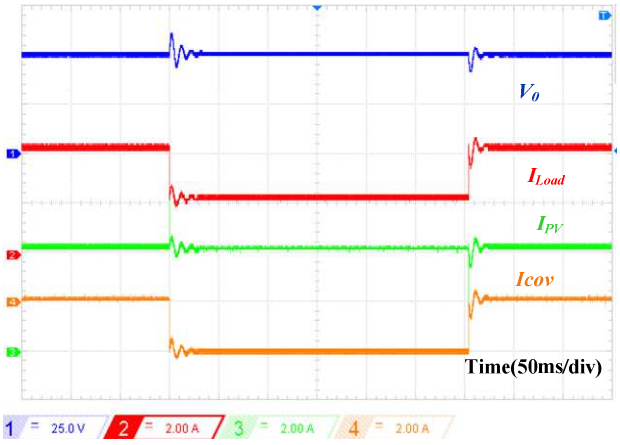

Fig. 8. Experimental results when load power is varied from 200W to 100W and vice-versa. (buck mode).

V. Conclusion

An efficient control strategy, known as FF-ISMC, has been enacted for BSQZSDC as a result of this paper. Energy management between the photovoltaic panel, the battery, and the load can be achieved in both the buck and boost modes. The controller, and converter operation in both the charge (buck) and discharge (boost) modes was analysed in depth. The controller was able to meet all of the requirements for such regulation of the battery's voltage and current. Further, the experimental validation of the on BSQZSDC is executed.

VI References

[1] F. Z. Peng, "Z-source inverter," *IEEE Trans. Ind. Appl.*, vol. 39, no. 2, pp. 504–510, 2003.

[2] J. Anderson and F. Z. Peng, "Four quasi-Z-Source inverters," *PESC Rec. - IEEE Annu. Power Electron. Spec. Conf.*, pp. 2743–2749, 2008.

[3] M. Mohammadi, A. Mirzaee, J. S. Moghani, J. Milimonfared, and M. Zarei Tazehkand, "A quasi-Z-source inverter with a single high-frequency-switch," *Int. Trans. Electr. Energy Syst.*, vol. 31, no. 3, pp. 1–18, 2021.

[4] J. Liu, S. Jiang, D. Cao, and F. Z. Peng, "A digital current control of quasi-Z-source inverter with battery," *IEEE Trans. Ind. Informatics*, vol. 9, no. 2, pp. 928–937, 2013.

[5] Y. Raj Kafle, M. J. Hossain, and M. Kashif, "Quasi-Z-source-based bidirectional DC-DC converters for renewable energy applications," *Int. Trans. Electr. Energy Syst.*, vol. 31, no. 4, pp. 1–16, 2021.

[6] D. Vinnikov and I. Roasto, "Quasi-Z-Source-based isolated DC/DC converters for distributed power generation," *IEEE Trans. Ind. Electron.*, vol. 58, no. 1, pp. 192–201, 2011.

[7] H. Shen, B. Zhang, D. Qiu, and L. Zhou, "A Common Grounded Z-Source DC-DC Converter With High Voltage Gain," *IEEE Trans. Ind. Electron.*, vol. 63, no. 5, pp. 2925–2935, 2016.

[8] Y. Zhang, Q. Liu, J. Li, and M. Sumner, "A Common Ground Switched-Quasi-Z -Source Bidirectional DC-DC Converter with Wide-Voltage-Gain Range for EVs with Hybrid Energy Sources," *IEEE Trans. Ind. Electron.*, vol. 65, no. 6, pp. 5188–5200, 2018.

[9] S. Battula, M. Mohan Garg, A. Kumar Panda, M. Preetam Korukonda, and L. Behera, "Analysis and Dual-loop PI Control of Bidirectional Quasi Z-Source DC-DC Converter," *IECON Proc. (Industrial Electron. Conf.*, vol. 2020-Octob, pp. 2939–2944, 2020.

[10] M. M. Garg, Y. V. Hote, and M. K. Pathak, "PI controller design of a DC-DC Zeta converter for specific phase margin and cross-over frequency," *2015 10th Asian Control Conf. Emerg. Control Tech. a Sustain. World, ASCC 2015*, 2015.

[11] Y. He and F. L. Luo, "Sliding-mode control for dc-dc converters with constant switching frequency," *IEE Proc. Control Theory Appl.*, vol. 153, no. 1, pp. 37–45, Jan. 2006.

[12] Y. He and F. L. Luo, "Sliding-mode control for dc–dc converters with constant switching frequency," *Univ. Manitoba*, p. 144, 2001.

[13] Y.-M. Siew-Chong Tan, Lai and C. K. Tse, *Sliding Mode Control of Switching PowerConverters*, 2012th ed. Boca Raton,FL,USA: CRC Press, 2012.

[14] Y. Li, X. Ruan, L. Zhang, J. Dai, and Q. Jin, "Variable Switching Frequency ON-OFF Control for Class e DC-DC Converter," *IEEE Trans. Power Electron.*, vol. 34, no. 9, pp. 8859–8870, 2019.

[15] M. Gao, D. Wang, Y. Li, and T. Yuan, "Fixed Frequency Pulse-Width Modulation Based Integrated Sliding Mode Controller for Phase-Shifted Full-Bridge Converters," *IEEE Access*, vol. 6, pp. 2181–2192, 2017.

[16] S. C. Tan, Y. M. Lai, C. K. Tse, and M. K. H. Cheung, "A fixed-frequency pulsewidth modulation based quasi-sliding-mode controller for buck converters," *IEEE Trans. Power Electron.*, vol. 20, no. 6, pp. 1379–1392, 2005.

[17] J. Liu, S. Jiang, D. Cao, X. Lu, and F. Z. Peng, "Sliding-mode control of quasi-Z-source inverter with battery for renewable energy system," *IEEE Energy Convers. Congr. Expo. Energy Convers. Innov. a Clean Energy Futur. ECCE 2011, Proc.*, pp. 3665–3671, 2011.

[18] Y. Pan, C. Yang, L. Pan, and H. Yu, "Integral Sliding Mode Control: Performance, Modification, and Improvement," *IEEE Trans. Ind. Informatics*, vol. 14, no. 7, pp. 3087–3096, 2018.

[19] S. Battula, A. K. Panda, and M. M. Garg, "Design and Development of Fixed-Frequency Double-Integral SM-Controlled Solar-Integrated Bidirectional Quasi Z -Source DC-DC Converter in Standalone Battery Connected System," *Int. Trans. Electr. Energy Syst.*, vol. 2022, 2022.